Available online at http://www.ssstj.sci.ssru.ac.th

SSSTJ

**Suan Sunandha Science and Technology Journal**


# Conductive Composite Paper from Cellulose Fiber by in situ Polymerization of Pyrrole

**Siripassorn Sukhkhawuttigit[1*], Sarute Ummartyotin[2], Yingyot Infahsaeng[1**]**

[1] Division of Physics, Faculty of Science and Technology, Thammasat University, Klong Nueng, Klong Luang, Pathum-Thani, Thailand

[2] Division of Materials and Textile Technology, Faculty of Science and Technology, Thammasat University, Klong Nueng, Klong Luang, Pathum-Thani, Thailand

**Corresponding author e-mail**: ***ss.siripassorn@gmail.com****yingyot.infahsaeng.gmail.com**

**Received**: *6 January 2020* / **Revised:** *17 January 2020* /**Accepted**: *30 January 2020*

**Abstract**

Currently, conducting polymers such as Polypyrrole (PPy), have been extensively interested due to their interesting features of conductivity, low-cost fabrication, and stability under ambient conditions and at high temperature. Herein, polypyrrole was polymerized on the surface of cellulose fibers (CFs) by using a sequence of fiber impregnation in $FeCl_3$ solutions and re-dispersion in a pyrrole solution via in situ chemical polymerization of monomer-pyrrole. The structure, morphology, and thermal properties were investigated. The results revealed the uniformly of PPy on the surface of CFs. Moreover, conductivity of $184\times10^{-4}$ S·cm$^{-1}$ was obtained from a composites sheet of CFs:PPy with the PPy of 0.20 ml. Also, the decreasing of dielectric and impedance in CFs:PPy composites sheet can be observed as the increasing of CFs:PPy ratio. Chemical polymerization has been very successful in the production of composite materials of conductivity polymers with CFs.

**Keywords**: Polypyrrole, Conductive composite materials, in situ Synthesized

## 1. Introduction

Typically, the electronic devices were made of silicon, conductive glass or hard plastic, which is an importance part for high performance device, but such materials still have limitations in terms of brittleness, cost of materials and complex production processes. Moreover, some plastic, especially micro-plastic, is not environmental-friendly. Consequently, non-reused materials can lead to an environmental problem. To overcome this issue, bio-based materials have been developed under the concept of "green" and sustainable development, which can naturally decompose and pollution reduction. Therefore, the renewable natural materials are the important topic in the 21st century(Mohanty, Misra, & Drzal, 2002).

The development of alternative bio-based materials which has similar properties such as electrical, thermal, flexibility and mechanical properties, is crucial .Nowadays, the cellulose has been widely studied and developed due to its renewability, availability, non-toxicity, low-cost, biodegradability, thermal and chemical stability (Wang, Lu, & Zhang, 2016). One of the interesting developments of cellulose is conductive paper, which is very important for electronic device application such as TFT, OLED, organic photovoltaic device, stored battery, and sensor (Fu et al., 2016; Ummartyotin & Manuspiya, 2015a, 2015b). Recently, the conductive paper was successfully fabricated with a sheet resistance of 25 kΩ (Zhong et al., 2013).

To develop the conductive paper, conductive polymers are interesting material due to its unique properties that allow it to be used in a variety of electrical application. Typically, chemical polymerization has been successful in the production of composite materials of conductive polymers with the matrix. Recently, the conductive nanocrystal cellulose:polypyrrole composite hydrogel were in situ synthesized. By doping with sodium p-toluenesulfonate (TsONa), the hydrogel showed a high electrical conductivity of $8.8\times10^{-3}$ S/cm (Li, Zhang, & Xiao, 2018). Moreover, the effect of polypyrrole and ionic liquid (IL) nanocoatings on the electrical properties of cellulose film has been investigated. The conductivity of such nanocomposite film was $1.2\times10^{-4}$ and $4.3\times10^{-5}$ S/cm on the surface and along

the thickness direction, respectively (Mahadeva & Kim, 2011). Combination of bio-based materials such as cellulose with conductive polymer has been extensively developed as a multi-function electronic device (Du, Zhang, Liu, & Deng, 2017) . Recently, many researchers have extensively attended to develop such composite material. The organic or inorganic composite materials were a material that can be obtained from the combination of various materials to get new properties . To prepare the conductive composites of bacterial cellulose (BC) and polypyrrole, Muller and co-worker prepared through in situ oxidative chemical polymerization of pyrrole by using $FeCl_3$ as oxidant agent (Müller, Rambo, Recouvreux, Porto, & Barra, 2011). Makara and co-worker prepared nanopapers from cellulose nanofibers (CNF) and polypyrrole with high mechanical performance and with the electrical conductivity of $5.2\times10^{-2}$ S/cm (Lay, Méndez, Delgado-Aguilar, Bun, & Vilaseca, 2016). Pyrrole and cellulose are therefore an interesting material that shows the connection between cellulose fibers and conductive polymers. There were flexibility and capacitance properties that make it more useful in using technology.

In this work, the cellulose fiber obtained from the remaining pulp is mixed with polypyrrole (PPy) via in situ polymerization using ferric chloride as oxidant agent. An amount of PPy is varied, then the morphology, mechanical, and electrical properties are investigated.

## 2. Materials and Method

### 2.1. Materials

A wastepaper pulp was provided from SCG packaging public company limited, Thailand, and was stored in a desiccator in order to prevent the moisture adsorbent .Pyrrole was supplied by Sigma Aldrich and used as received for the chemical synthesis of polypyrrole . The rest of materials, $FeCl_3$ and HCl, were also supplied by Sigma Aldrich and used without further purification.

### 2.2. Method

- **Cellulose suspension**

The piece of paper pulp with an area of ca. 10x10 $cm^2$, was ripped to be a thin sheet. Then the pulp was mixed with deionized water DI of 500 ml for overnight under magnetic stirrer .The obtained suspension was concentrated and subsequently washed with distilled water by repeated centrifuged cycles at 500 rpm. As a result, suspension of cellulose fiber (CFs) was obtained and stored at 4 $^{o}$C prior to use.

- **Preparation of Cellulose fiber (CFs) and CFs:PPy paper**

CFs suspension of 45 ml (0.4 g dry weight) was dispersed in 30 ml of HCl and stirred by for 5 minutes. After that, the CFs suspension was filtered for 24 hr through a paper filter with 0.1 $\mu$m pore size and washed subsequently with DI water. The wet sheet was then dried between two membranes under an applied pressure of 0.141 psi.

For the preparation of CFs:PPy paper, the various volume of pyrrole solution (0.05, 0.10, 0.15, 0.20 ml )was dissolved in 30 ml of 0.5M HCl and, then, mixed with the CFs dispersion and stirred for 5 minutes. A defiant amount of $FeCl_3$ was dissolved in 30 ml aqueous of 0.5M HCl solution and added to the CFs:pyrrole dispersion to initiate oxidative polymerization . The oxidant ($FeCl_3$) to pyrrole was fixed at 6 %w/w ratio. The final mixture was stirred at room temperature for 30 minutes. At the end, the mixture was filtered using paper filter and washed subsequently 30 ml of 0.5M HCl and DI water to remove any small gas bubbles and to allow a better organization of CFs:PPy structures without undesired side effects, such as crystal structure damage (Ali et al., 2014).

**Suan Sunandha Science and Technology Journal**


### 2.3. Characterizations

- **Fourier Transform Infrared Spectroscopy (FTIR)**

FTIR absorption spectra (PerkinElmer, spectrum 100) of cellulose and CFs:PPy composites were recorded in the range of 4000 $cm^{-1}$ to 650 $cm^{-1}$ using Attenuated Reflection Infrared Spectroscopy (ATR) mode (Pleumphon, Thiangtham, Pechyen, Manuspiya, & Ummartyotin, 2017).

- **X-Ray Diffractometer (XRD)**

X-ray diffraction patterns of CFs, CFs:PPy composites were carried out by X-Ray Diffractometer (Bruker, D8 ADVANCE) using Co radiation at 40 kV voltage. The XRD patterns were recorded in a diffraction angle (2θ) range from 5° to 50° (ElNahrawy, Haroun, Hamadneh, & Al-Dujaili, 2017).

- **Thermogravimetric Analysis (TGA)**

The TGA characteristics of the CFs:PPy composite were investigated by TGA (MET-TLER TOLEDO, TGA/DSC3+1600). Each sample was heated at a heating rate of 10 °C/min under nitrogen atmosphere from room temperature to 700 °C (Pleumphon et al., 2017).

- **Field Emission Scanning Electron Microscope (FE-SEM)**

The morphological properties of the CFs and CFs:PPy composite were analyzed using FE-SEM (Hitachi, S-4800) at an acceleration voltage of 5 kV. The fiber diameter was measured and counted at 1000x magnification. Prior to the investigation, the samples were stored in desiccators to reduced humidity. Each sample was placed on carbon tape and sputtered with gold particles before being analyzed (Pleumphon et al., 2017)

- **Mechanical properties**

The sample was cuter into the rectangle shape with the width of 20 mm and length of 30 mm. The thickness of sample was ca. 0.07 - 0.09 mm. The testingspeed was 5 mm/min. The tensile tests were conducted using as Instron Universal material testing machine (Instron 55R4502, S/NH 3342) equipped with a 100 N load cell (Pleumphon et al., 2017).

- **Conductivity**

The conductivity properties of CFs:PPy substrate was characterized by Four Point Probe System (Jandel RM3000) using the cylindrical four-point probe head (Du et al., 2017).

- **Dielectric and Impedance**

Impedance were measured using an impedance probe (1260 Impedance Gain-Phaze Analyzer 12600012_Gmacd/CB Solartron) at room temperature and at various frequencies ranging from 10 Hz to 10 MHz (Jandel Engineering Limited) (ElNahrawy et al., 2017; Raghunathan, Narayanan, Poulose, & Joseph, 2017)

## 3. Results and discussion

### 3.1. FTIR analysis

The FTIR spectra of CFs and CFs:PPy composites are shown in Figure 1. The spectrum of the prepared CFs show the peaks at 3335.69 $cm^{-1}$ which is the characteristic for stretching vibration of the hydroxyl group (O-H group) in polysaccharides (Rosa et al., 2010). The peak located at 1633 $cm^{-1}$ correspond to stretching vibrations of C-C bonds (Poletto, Pistor, Zeni, & Zattera, 2011). The absorption bands at 1377.85, 1250.26, 1161.10, 1052.43, and 897.03 $cm^{-1}$ belong to stretching and bending vibrations of $-CH_2$, -CH, -OH and C-O bonds in cellulose, respectively (Fackler et al., 2011; Xu, Yu, Tesso, Dowell, & Wang, 2013). From FTIR spectra of CFs:PPy composites at different PPy concentration, it was observed that the peak 3277 $cm^{-1}$ was shifted from 3335.69 $cm^{-1}$, this may be due to chemical bonding between N-H in the polypyrrole ring and the –OH of cellulose (Müller et al., 2011). The fundamental vibrations of pyrrole ring observed at 1541.08 $cm^{-1}$ and 1458 $cm^{-1}$, which can be assigned to the C=C and C-C ring stretching modes, respectively (Chougule et al., 2012; Hansora, Shimpi, & Mishra, 2015). The peak around 1046 $cm^{-1}$ can be assigned to N-H in-plane deformation (Ho, Jun, & Kim, 2013), while the peak at 781 $cm^{-1}$ is due to C-N out-of-plane deformation in PPy (Chougule et al., 2012).The absorption peak at about 1125-1159 $cm^{-1}$ and 883.68 $cm^{-1}$ may be relate



Vol.07, No.1 DOI:10.14456/ssstj.2020.4

**Suan Sunandha Science and Technology Journal**


to linkage between polypyrrole and cellulose chain in 1161.10 $cm^{-1}$ and 867.03 $cm^{-1}$.

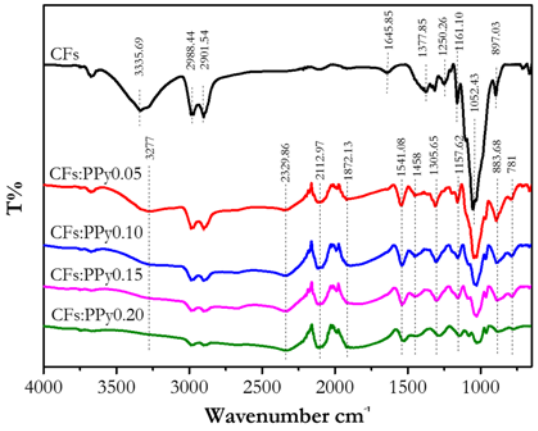


**Figure 1**. FTIR spectra of CFs and CFs:PPy composites.

### 3.2. Crystallography structures

The crystallography structures of CFs and CFs:PPy composites were characterized using XRD measurements as shown in Figure 2 .The X-ray pattern clearly exhibits the broaden peaks at 2θ of 16° and 22° for both CFs and CFs:PPy composite. The clearly peaks can be assigned to the crystalline structure of cellulose (Ford, Mendon, Thames, & Rawlins, 2010). Also, the broaden characteristic of various CFs:PPy composites were exhibited in the region of 15° - 25° which is the amorphous phase of polypyrrole (Luo et al., 2010).

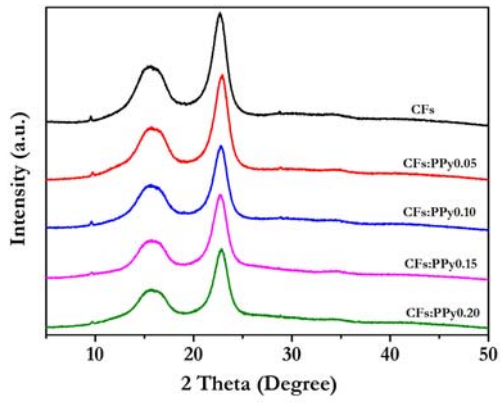


**Figure 2**. XRD patterns of CFs and CFs:PPy composites.

### 3.3. Thermogravimetric analysis

The degradation temperatures of CFs and CFs:PPy papers were studied by thermogravimetric analysis as shown in Figure 3. CFs and CFs:PPy showed main weight loss in three stages. For CFs, it demonstrates that the thermal stability of the prepared CFs in much higher than that of composites in the temperature lower than 250 ℃. As composite is hygroscopic, nearly 8% weight loss is occurred at 100 ℃. The second stage of weight loss started at 250 ℃ and continued up to 500 ℃ with rapidly 80% of weight loss. The last stages of temperature at > 500 ℃ almost 100% of weight loss can be observed for all conditions. For CFs:PPy composites, the first stage range between room temperature and 250 ℃ showed about a 13% of weight loss. The second stage of weight loss started at 250 ℃ and continued up to 500 ℃ during which there was nearly an 80% of gradually weight loss. The last states of temperature up to 500 ℃ during which there was a 100% of weight loss. From the above analysis, it clearly shows that the thermal stability of CFs was greatly affected by incorporating PPy. The incorporated PPy lowered the starting thermal degradation of CFs.

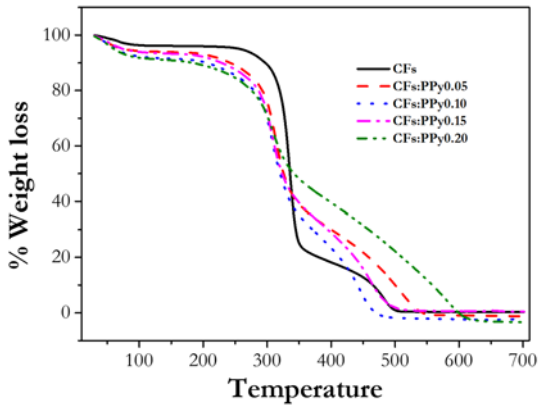


**Figure 3**. TGA of CFs and CFs:PPy composites.

### 3.4. FE-SEM analysis

The morphology of CFs, CFs:PPy composites was studied using Field Emission Scanning Electron Microscope as shown in Figure 4. The Figure 4 (a) shown that the CFs surface is rather straight and smooth without the formation of cross-link between fiber. It is important to note that CFs appears to be a



Vol.07, No.1 DOI: 10.14456/ssstj.2020.4

**Suan Sunandha Science and Technology Journal**


uniform fibrous network. For CFs:PPy composites as shown in Figure 4 (b-e), the formation of PPy on the CFs in the form of clusters and cross-link between fiber network can be observed (ElNahrawy et al., 2017), which involving the formation of H-bonds between the cellulose and the polypyrrole chain. These interactions were a result of both intermolecular and intramolecular forces, causing the composites sheet to be less cellulose fiber density.

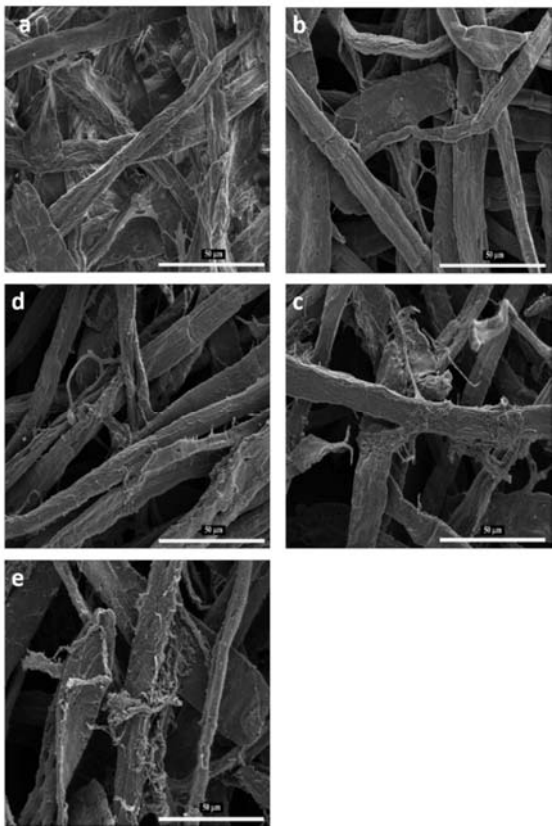


**Figure 4**. FE-SEM of composite materials with different pyrrole preparation condition (a) CFs (b) CFs:PPy0.05 (c) CFs:PPy0.10 (d) CFs:PPy0.15 (e) CFs:PPy0.20.

### 3.5. Mechanical properties

The tensile strength, Young's modulus, and elongation at break of neat CFs and CFs:PPy composite were presented in Table 1. Not surprisingly, tensile strength and young's modulus were decreased as the increasing of PPy additive. This effect may be caused by the inter-percolation of PPy between CFs network. However, the elongation at break of composite is not dramatically reduced, when increasing the amount of additive. After the polymerization process of pyrrole, PPy network may be grouped to be clusters which can be observed from the SEM image. Therefore, PPy network was poorly dispersed into cellulose fibers matrix by present preparation.

**Table 1**. Mechanical properties of CFs and CFs:PPy composites.

| Sample | Tensile strength (MPa) | Young's modulus (MPa) | Elongation at break (%) |
|---|---|---|---|
| CFs | 2.038±0.761 | 248.940±85.926 | 1.404± 0.440 |
| CFs:PPy0.05 | 0.798±0.520 | 109.652±871.73 | 1.180±0.234 |
| CFs:PPy0.10 | 0.554±0341 | 109.858±68.977 | 0.698±0.119 |
| CFs:PPy0.15 | 0.213±0.285 | 39.715±53.154 | 0.868±0.331 |
| CF:PPy0.20 | 0.026±0.020 | 2.962±3.546 | 1.524±0.389 |

### 3.6. Conductivity properties

The electrical conductivities of CFs:PPy composites with different amount of PPy were measured using a four-point probe technique. Table 2 shows the sheet resistance, resistivity, and electrical conductivities of CFs:PPy composites. The experimental setup and parameters calculation are described in literature (J. Li, Wang, & Ba, 2012). The CFs has basically no conductivity, while the resistance and resistivity of CFs:PPy composites decrease as the increasing of PPy additive. Consequently, the electrical conductivities of CFs:PPy composites are increased up to $1.84 \times 10^{-2}$ S/cm at 0.20 ml PPy. Compare to the conductivity of typically semiconductor ($10^{-7}$–$10^{5}$ S/cm), the conductivity of CFs:PPy is in a range of promising application of electronic device.



Vol.07, No.1 DOI:10.14456/ssstj.2020.4

**Suan Sunandha Science and Technology Journal**


**Table 2**. Conductivity of the CFs and CFs:PPy composites.

| Sample | Resistance (Ω) x10$^3$ | Resistivity (Ωm) x10$^3$ | Conductivity (S·cm$^{-1}$)x10$^{-4}$ |
|---|---|---|---|
| CFs | - | - | - |
| CFs:PPy(0.05) | 10.7±0.742 | 67.4±4.66 | 1.49±0.106 |
| CFs:PPy(0.10) | 1.19±0.0944 | 7.51±0593 | 13.3±1.05 |
| CFs:PPy(0.15) | 0.735±0.0792 | 4.62±0.498 | 21.9±2.44 |
| CFs:PPy(0.20) | 0.0938±0.0241 | 0.589±0.151 | 184±58.9 |

### 3.7. Dielectric properties

Figure. 5. Shows dielectric properties of CFs and CFs:PPy composite materials. Typically, the dielectric properties of polymer composites can be affected by the polymer type or dopant type. The variation of dielectric constant (permittivity, ε′) and loss tangent as a function of frequency for the prepared samples with different composition of PPy are presented. The dielectric constants were very high at low frequency and were slightly decreased when the frequency increased. Note that the dielectric constant of CFs is more rapidly decreased when comparing to that of CFs:PPy composites. The reducing of dielectric constants can be expressed by the relaxation behavior. With high region of frequency, the charge has insufficient time of re-orientation under applied external field and it was therefore presented as a lower of dielectric properties. In addition, the loss tangent of CFs and CFs:PPy composite is not significantly difference.

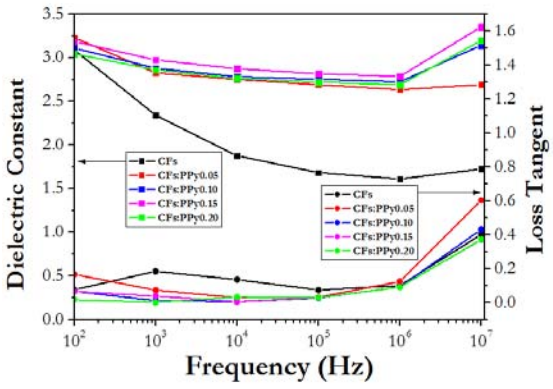


**Figure 5**. Variation of dielectric constant and loss tangent of CFs and CFs:PPy composites with frequency.

### 3.8. Impedance properties

Figure. 6. Shows the complex impedance spectra with the variation of the imaginary part of the complex impedance (Z″) versus its real part (Z′). The frequency range was from 10 Hz to 10 MHz and the applied AC signal was 0.5 V. The impedance spectra are characterized as semicircle, which is most probably result of the facilitated transport of the doping anions in the bulk of the composites. The transport of the doping anions can be enhance by increasing the amount of PPy (Nakata & Kise, 1993; Porjazoska Kujundjiski, Chamovska, & Grchev, 2014). The best fit of experimental data to model was obtained using a constant phase element (CPE) rather than an ideal capacitor. The equivalent circuit model is shown in Figure 6. The best fit of experimental data to model was obtained using a constant phase element (CPE) rather than an ideal capacitor. The capacitance of $3.168\times10^{-11}$ F can be obtained from the composites at 0.20 ml PPy. The equivalent circuit model is shown in Figure 6.

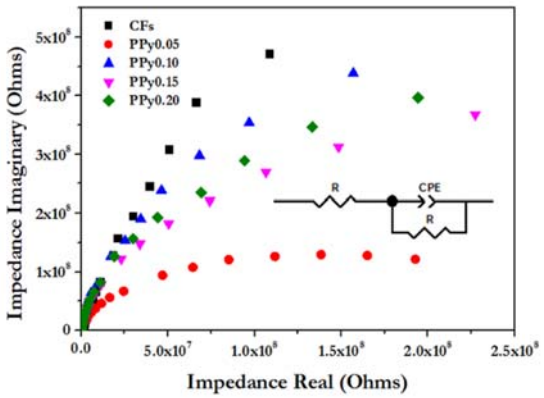


**Figure 6**. Figure 6. Impedance spectra of CFs and CFs:PPy composites.

## 4. Conclusions

A cellulose paper was demonstrated with the aid of in situ synthesized conductive cellulose (CFs):polypyrrole (PPy) network. Chemical polymerization has been very successful in the production of composite materials of conductivity polymers with CFs. Increasing polypyrrole content in the composite affected the features of cellulose. The morphology of CFs exhibited a very straight and smooth surface. When PPy was composited with



Vol.07, No.1 DOI:10.14456/ssstj.2020.4

**Suan Sunandha Science and Technology Journal**


CFs, the PPy clusters were formed on the CFs. Increasing of the PPy amount causes the reduction of mechanical properties due to interpercolation of PPy in cellulose. Also, the decreasing of dielectric and impedance in CFs:PPy composites sheet can be observed as the increase of CFs:PPy ratio. Moreover, conductivity of $184\times10^{-4}$ S/cm was obtained from a composites sheet of CFs:PPy (0.20).

## 5. Acknowledgement

The authors would like to thank for the financial support provided by Thammasat University under the National Research Council of Thailand (NRCT)

## 6. Publication Ethic

Submitted manuscripts must not have been previously published by or be under review by another print or online journal or source.

## 7. References

Ali, F., Reinert, L., Lévêque, J.-M., Duclaux, L., Muller, F., Saeed, S., & Shah, S. S. (2014). Effect of sonication conditions: solvent, time, temperature and reactor type on the preparation of micron sized vermiculite particles. *Ultrasonics sonochemistry, 21*(3), 1002-1009. doi: 10.1016/j.ultsonch.2013.10.010

Chougule, M., Dalavi, D., Mali, S., Patil, P., Moholkar, A., Agawane, G., . . . Patil, V. (2012). Novel method for fabrication of room temperature polypyrrole–ZnO nanocomposite NO2 sensor. *Measurement, 45*(8), 1989-1996. doi: 10.1016/j.measurement.2012.04.023

Du, X., Zhang, Z., Liu, W., & Deng, Y. (2017). Nanocellulose-based conductive materials and their emerging applications in energy devices-A review. *Nano Energy, 35*, 299-320. doi:10.1016/j.nanoen.2017.04.001

El Nahrawy, A. M., Haroun, A. A., Hamadneh, I., & Al-Dujaili, A. H. (2017). Conducting cellulose/$TiO_2$ composites by in situ polymerization of pyrrole. *Carbohydrate polymers, 168*, 182-190. doi: 10.1016/j.carbpol.2017.03.066

Fackler, K., Stevanic, J. S., Ters, T., Hinterstoisser, B., Schwanninger, M., & Salmén, L. (2011). FT-IR imaging microscopy to localise and characterise simultaneous and selective white-rot decay within spruce wood cells. *Holzforschung, 65*(3), 411-420.

Ford, E. N. J., Mendon, S. K., Thames, S. F., & Rawlins, J. W. (2010). X-ray diffraction of cotton treated with neutralized vegetable oil-based macromolecular crosslinkers. *Journal of Engineered Fibers and Fabrics, 5*(1), 155892501000500102. doi:10.1177/155892501000500102

Fu, J., Zhang, J., Song, X., Zarrin, H., Tian, X., Qiao, J., . . . Chen, Z. (2016). A flexible solid-state electrolyte for wide-scale integration of rechargeable zinc–air batteries. *Energy & Environmental Science, 9*(2), 663-670. doi:10.1039/c5ee03404c

Hansora, D., Shimpi, N., & Mishra, S. (2015). Graphite to graphene via graphene oxide: an overview on synthesis, properties, and applications. *Jom, 67*(12), 2855-2868. doi: 10.6084/m9.figshare.1094371

Ho, T. A., Jun, T.-S., & Kim, Y. S. (2013). Material and $NH_3$-sensing properties of polypyrrole-coated tungsten oxide nanofibers. *Sensors and Actuators B: Chemical, 185*, 523-529. doi:10.1016/j.snb.2013.05.039

Lay, M., Méndez, J. A., Delgado-Aguilar, M., Bun, K. N., & Vilaseca, F. (2016). Strong and electrically conductive nanopaper from cellulose nanofibers and polypyrrole. *Carbohydrate polymers, 152*, 361-369. doi:10.1016/j.carbpol.2016.06.102

Li, J., Wang, Y., & Ba, D. (2012). Characterization of semiconductor surface conductivity by using microscopic four-point probe technique. *Physics Procedia, 32*, 347-355. doi: 10.1016/j.phpro.2012.03.568

Li, Y., Zhang, H., Ni, S., & Xiao, H. (2018). In situ synthesis of conductive nanocrystal cellulose/polypyrrole composite hydrogel based on semi-interpenetrating network. *Materials Letters, 232*, 175-178.

Luo, Y.-L., Fan, L.-H., Xu, F., Chen, Y.-S., Zhang, C.-H., & Wei, Q.-B. (2010). Synthesis and characterization of $Fe_3O_4$/PPy/P (MAA-co-AAm) trilayered composite microspheres with electric, magnetic and pH response characteristics. *Materials Chemistry and Physics, 120*(2-3), 590-597.

Mahadeva, S. K., & Kim, J. (2011). Enhanced electrical properties of regenerated cellulose by polypyrrole and ionic liquid nanocoating. *Proceedings of the Institution of Mechanical Engineers, Part N: Journal of Nanoengineering and Nanosystems, 225*(1), 33-39. doi:10.1177/1740349911404100

Mohanty, A. K., Misra, M., & Drzal, L. (2002). Sustainable bio-composites from renewable resources: opportunities and challenges in the green materials world. *Journal of Polymers and the Environment, 10*(1-2), 19-26.

Müller, D., Rambo, C., Recouvreux, D., Porto, L., & Barra, G. (2011). Chemical in situ polymerization of polypyrrole on bacterial cellulose nanofibers. *Synthetic Metals, 161*(1-

**Suan Sunandha Science and Technology Journal**


2),106-111. doi:10.1016/j.synthmet.2010.11.005

Nakata, M., & Kise, H. (1993). Preparation of Polypyrrole-Poly(vinyl chloride) Composite Films by Interphase Oxidative Polymerization. *Polymer Journal, 25*(1), 91-94. doi:10.1295/polymj.25.91

Pleumphon, C., Thiangtham, S., Pechyen, C., Manuspiya, H., & Ummartyotin, S. (2017). Development of conductive bacterial cellulose composites: An approach to bio-based substrates for solar cells. *Journal of Biobased Materials and Bioenergy, 11*(4), 321-329.doi: 10.1166/jbmb.2017.1686

Poletto, M., Pistor, V., Zeni, M., & Zattera, A. J. (2011). Crystalline properties and decomposition kinetics of cellulose fibers in wood pulp obtained by two pulping processes. *Polymer Degradation and Stability, 96*(4), 679-685. doi:10.1016/j.polymdegradstab.2010.12.007

Porjazoska Kujundjiski, A., Chamovska, D., & Grchev, T. (2014). Capacitive properties of polypyrrole/activated carbon composite. *Hemijska industrija, 68*, 63-63. doi:10.2298/HEMIND140305063P

Raghunathan, S. P., Narayanan, S., Poulose, A. C., & Joseph, R. (2017). Flexible regenerated cellulose/polypyrrole composite films with enhanced dielectric properties. *Carbohydrate polymers, 157*, 1024-1032. doi: 10.1016/j.carbpol.2016.10.065

Rosa, M., Medeiros, E., Malmonge, J., Gregorski, K., Wood, D., Mattoso, L., . . . Imam, S. (2010). Cellulose nanowhiskers from coconut husk fibers: Effect of preparation conditions on their thermal and morphological behavior. *Carbohydrate polymers, 81*(1), 83-92. doi: 10.1016/j.carbpol.2010.01.059

Ummartyotin, S., & Manuspiya, H. (2015a). A critical review on cellulose: from fundamental to an approach on sensor technology. *Renewable and Sustainable Energy Reviews, 41*, 402-412. doi: 10.1016/j.rser.2014.08.050

Ummartyotin, S., & Manuspiya, H. (2015b). An overview of feasibilities and challenge of conductive cellulose for rechargeable lithium based battery. *Renewable and Sustainable Energy Reviews, 50*, 204-213. doi:10.1016/j.rser.2015.05.014

Wang, S., Lu, A., & Zhang, L. (2016). Recent advances in regenerated cellulose materials. *Progress in Polymer Science, 53*, 169-206. doi:10.1016/j.progpolymsci.2015.07.003

Xu, F., Yu, J., Tesso, T., Dowell, F., & Wang, D. (2013). Qualitative and quantitative analysis of lignocellulosic biomass using infrared techniques: a mini-review. *Applied Energy, 104*,801-809. doi:10.1016/j.apenergy.2012.12.019

Zhong, Q., Zhong, J., Hu, B., Hu, Q., Zhou, J., & Wang, Z. L. (2013). A paper-based nanogenerator as a power source and active sensor. *Energy & Environmental Science, 6*(6), 1779-1784. doi: 10.1039/c3ee40592c